SPECIAL ISSUE PAPER

Analytical Performance Estimation of Network-Assisted D2D Communications in Urban Scenarios with Rectangular Cells

Andrey Samuylov[1], Aleksandr Ometov[1]*, Vyacheslav Begishev[2], Roman Kovalchukov[1], Dmitri Moltchanov[1], Yuliya Gaidamaka[2], Konstantin Samouylov[2], Sergey Andreev[1], and Yevgeni Koucheryavy[1]

[1] Tampere University of Technology, Korkeakoulunkatu 10, FI-33720, Finland
[2] Peoples' Friendship University of Russia, Ordzhonikidze str. 3, 115419, Russian Federation

ABSTRACT

The aggressive spatial reuse of radio resources is considered today as one of the most promising avenues to achieve significant cellular capacity improvements in future 5G networks. Accordingly, device-to-device (D2D) communications is an emerging paradigm that promises to offer these much expected gains without the need for additional investments into the network infrastructure. However, before this attractive technology can be deployed ubiquitously, the research community has to fully understand the extent of its potential performance benefits across typical scenarios of interest. In this work, we consider one such use case of rectangular cells (common for offices, shopping malls, dormitories, etc.) and develop the corresponding analytical methodology for D2D performance evaluation. As our target metric, we employ the signal-to-interference (SIR) ratio experienced by a D2D user. To this end, we propose two relatively simple approximations for SIR distribution and hence capture the related parameters, including user throughput. Further, we carefully investigate the most interesting numerical results by making important conclusions on the envisioned operation of our chosen scenario. In particular, we demonstrate that under certain conditions the SIR behavior is insensitive to the dimensions of cells, while different propagation exponents "scale" its density function thus allowing to simplify the characterization of SIR in a wide range of input parameters. Copyright © 2017 John Wiley & Sons, Ltd.

*Correspondence
Aleksandr Ometov, TG414, Tampere University of Technology, Korkeakoulunkatu 10, FI-33720, Finland
E-mail: aleksandr.ometov@tut.fi

1. INTRODUCTION AND MOTIVATION

1.1. Challenges of 5G networking

During the last decade, the volume of traffic transmitted over the wireless networks has increased tremendously comparing to the previous years. According to Cisco forecasts, the corresponding increase rate in 2014 has been over 70% [1] and it is only expected to grow further. This is due to the maturity of the *fourth-generation* (4G) mobile broadband technology bringing decisive improvements in many aspects of cellular networking across a number of novel user applications and services. In particular, 4G has dramatically augmented the available access data rates at the same time enabling a rich set of advanced Internet services, thus effectively competing with other types of wireless solutions including WiFi [2].

The said significant increase in the air interface capacity indicates the beginning of the new era of truly ubiquitous Internet access and many believe that even the latest 4G systems would not be able to handle the resulting traffic avalanche in the very near future [3]. Furthermore, this trend is likely to continue with the advent of smart unattended devices accessing the next-generation cellular systems, which are projected to reach the unprecedented number of 50 billion connected "things" by 2020 [4]. Such

1

massive connectivity should, in turn, impact severely the user quality-of-service (QoS) levels as well as add to the shortage in the available network capacity [5].

An emerging response to the above developments is the deployment of denser pico- and femto-cells with smaller coverage areas [6, 7]. This could potentially provide the much needed improvements in user data rates and energy efficiency of various wireless devices [8, 9]. However, additional challenges arise along the lines of interference mitigation between such diverse smaller cells. In addition to the interference aspects, the cellular industry would need to handle higher rental fees together with the increased deployment and service costs [10]. Nevertheless, the trend for network densification is regarded today as a mainstream solution to upgrade the degrees of spatial reuse and thus meet the steadily growing traffic demand in the *fifth-generation* 5G systems.

In today's wireless networks, a significant proportion of traffic is produced by the peer-to-peer (P2P) applications and services that feature users communicating in close proximity [11, 12]. From this perspective, the reliance on direct device-to-device (D2D) transmissions in future 5G networks may be regarded as another form of densification – not with the infrastructure-based equipment, but rather with opportunistic user-based small "cells". Existing short-range radio technologies (e.g., WiFi) may already be used to enable D2D services by taking advantage of the lower-to-the-ground links with no need for additional infrastructure deployment costs. Therefore, D2D communications may be preferred whenever possible to offload P2P traffic between the neighboring users and thus avoid the use of a more expensive cellular resource [13]. Therefore, D2D connectivity is becoming an effective enabler to reach the target capacity goals in addition to the network congestion mitigation within the emerging 5G ecosystem [14].
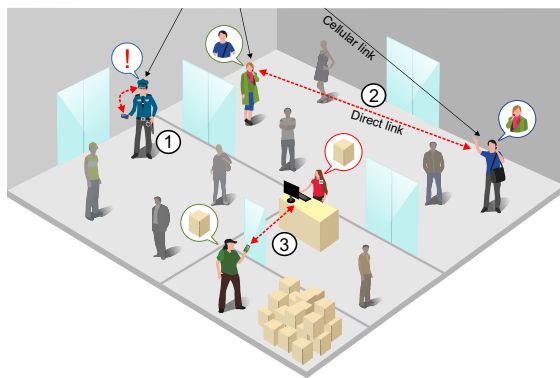

Figure 1. A typical urban D2D communications scenario.

In light of the above, direct connectivity promises to deliver such benefits as: (i) higher data rates, (ii) lower data transfer latencies, and (iii) better energy efficiencies to the proximate mobile devices [15]. Ultimately, the 5G network capacity has to grow by 1000x before 2020 and D2D communications is an attractive technology to reach

this ambitious goal. Therefore, both industry and academia are currently investigating this promising innovation to efficiently leverage the proximity gains in prospective 5G deployments. To this end, the dense urban scenarios shown in Fig. 1 are typically of interest. Here, use case ① corresponds to the critical public safety communications [16] and wearable connectivity [17], application ② is characteristic of video/audio session offloading [18], whereas context-aware, commercial, gaming, and other services are summarized by scenario ③ [19]. Below we continue with discussing the key performance factors that are behind most of these important D2D use cases.

1.2. Performance metrics and our focus

The signal-to-interference ratio (SIR) is the primary metric that characterizes the link quality between the communicating D2D users and thus reflects their ultimate throughput performance via the Shannon's law. In particular, SIR can be regarded as a proportion between the useful energy and that resulting from interference [20]. Due to the mobile and opportunistic nature of D2D connections, SIR is often a function of the current user location and, hence, can be treated as a random variable [21]. Correspondingly, SIR depends on the distance between the D2D transmitter and the respective receiver as well as on the set of active transmitters operating over a channel of interest. In other words, SIR at the receiving device indicates the extent of how much the effective signal is superior over various detrimental effects.

In this work, we target to analyze the SIR in a characteristic D2D scenario. The environment of interest consists of adjacent *rectangular* cells of certain dimensions [22], with D2D partners uniformly distributed across these cells. By concentrating on two adjacent cells and assuming that at most one D2D pair can be active in a particular cell at any given instant of time, we apply the methods coming from stochastic geometry to develop a comprehensive mathematical framework. Our employed technique thus offers a set of useful approximations for the characteristic D2D performance. In particular, these allow obtaining the integral expressions for the distributions of SIR and, therefore, all necessary moments and quantiles. Moreover, our framework may be easily extended to capture the actual throughput received by the D2D users in the considered scenario.

In a nutshell, our results demonstrate that (i) the scenario in question is insensitive to the dimensions of cells, as long as they have square shapes, while the propagation paths are characterized by the same attenuation, as well as (ii) the SIR distribution scales well when different propagation exponents are considered. These two observations allow to significantly simplify the SIR analysis in the considered and similar scenarios. Our developed framework also helps investigate the impact of the material of walls between the cells of interest on the resulting SIR. Essentially, the additional interference degradation due to the properties of the construction materials determines the

number of walls that the radio signal can penetrate. For instance, the walls made of steel or concrete cause more attenuation to the transmitted signal, which is reflected in our respective findings.

The rest of this text is organized as follows. Section 2 is devoted to a more detailed overview of the emerging D2D communications paradigm. Further, in Section 3 we introduce our considered system model and its main assumptions. The mathematical formulations behind the proposed D2D performance estimates are then developed in Section 4. The key numerical results of our system-level analysis are provided in Section 5. Finally, the conclusions are summarized in the last section.

2. BACKGROUND ON D2D COMMUNICATIONS

Recently, as part of the *Long Term Evolution* (LTE) cellular system development, various D2D connectivity mechanisms have been intensively investigated by the *Third Generation Partnership Project* (3GPP). As a consequence, the relevant standardization support is underway (coming in Release-12 and continued by Release-13) for a D2D technology operator to achieve efficient spatial reuse as well as provide proximal services and applications in future LTE deployments [23]. Originally, the pioneering idea has been to enable D2D communications over the licensed cellular spectrum in the *underlay* mode [24] and since then an extensive body of literature has accumulated on this subject.

2.1. Enabling D2D technologies

Generally, D2D underlay operates on the same resources as the cellular network itself and a prominent candidate technology for the *licensed-band* D2D is often nicknamed as *LTE-Direct*. Essentially, the related concept has been proposed several years ago in [25] for the P2P partners in close proximity to exchange data over a direct link while sharing spectrum with the conventional cellular users. With this prospective technology, mobile devices outside the cellular network coverage area may be able to communicate efficiently similar to how Terrestrial Trunked Radio (TETRA) technology [26] supports the scenarios of national security and public safety [27].

Importantly, *network-assisted* direct communications in licensed spectrum was originally proposed to improve the spatial reuse efficiency and reduce the user energy consumption opportunistically [28]. By designing and utilizing an appropriate cellular network control function, which offers possibilities for system-wide scheduling and synchronization, D2D partners receive additional performance benefits [29, 30]. In case of LTE-Direct, for example, the excessive interference may be mitigated by the introduction of novel D2D-aware power control methods, where the D2D partners manage their transmit powers to suppress the resultant interference to the cellular users [31]. To this

end, network-assisted licensed-band D2D communications is becoming an attractive area of investigation. However, despite the considerable research progress in this field [32], the corresponding standardization efforts are not developing at a fast pace resulting in the advent of several alternative near-term solutions before the D2D underlay technology finally meets the market.

As a viable second option, *unlicensed-band* direct connectivity promises to leverage the attractive D2D benefits almost immediately, as the respective short-range *WiFi-Direct* technology is already implemented in most contemporary mobile devices [33]. The main advantage of employing WiFi-Direct for D2D connectivity is so that this solution does not utilize the valuable licensed spectrum. However, unlicensed-band communications is historically subject to uncontrolled interference due to the lack of centralized power and channel access control. These can be made available to D2D partners with moderate degrees of cellular network assistance. As a result, proximal users would only connect over WiFi-Direct when actually required to transmit relevant data, while keeping their power-hungry short-range radios in idle at all other times by relying on ubiquitous cellular control. This simple yet efficient technology has already been made to work reliably and may be useful in the longer run as part of the 5G-grade D2D technology portfolio. More detailed information about possible D2D offloading solutions could be found in our recent work [34].

In summary, today there is still no universal standard for the centralized control over the D2D communications [35]. Another challenge at the stage of proximal discovery is the lack of suitable information security enablers [36]. However, we firmly believe that the remaining open research questions can all be solved promptly by further developing the network-assisted D2D solutions.

2.2. Related modeling work

Historically, when assessing user performance in conventional cellular networks, the major challenge has been associated with the uncertainty in the device position. Indeed, as today's user devices are typically mobile, their current geographical location with respect to the serving base station may change dynamically, which calls for the utilization of probabilistic methods to yield respective conclusions on the expected QoS levels. To make matters worse, in the emerging D2D-enabled cellular systems the challenge shifts to accounting for the uncertainty in the locations of all the involved D2D partners, given that both the transmitter and the receiver may be mobile.

To this end, there are two capable methodologies to potentially capture the resulting D2D performance – the optimization theory and the stochastic geometry. The *optimization theory* produces a system-wide "snapshot" at a certain time instant and helps develop practical algorithms for the optimized network operation, mindful of a given metric of interest. The distribution of users is often assumed to be random but fixed to a certain "typical"

realization of points on the plane. Then, after multiple iterations the uncertainty in user locations can be resolved satisfactorily. However, owing to numerous details that have to be taken into account as well as to the integer nature of the involved parameters, the resulting formulations appear as (mixed) integer programming (MIP) problems, which cannot be solved in polynomial time. Some feasible solutions may still be possible by applying game-theoretic models [37]. Ultimately, the major limitation of the described approach for the evaluation of the prospective D2D-enabled cellular systems is in its "fixed" nature of randomness, which requires time-consuming system-level simulations to deliver the target performance parameters.

Over the recent years, the *stochastic geometry* has become another extremely useful and popular tool for the analysis of various cellular systems. This methodology naturally considers a certain random distribution of users on the plane allowing to quantify their various performance parameters as functions of distance between the communicating entities. Not surprisingly, numerous research results capturing the distributions and the moments of SIR, Shannon capacity, spectral efficiency, and the actual data rate of users have emerged lately for a plethora of interesting scenarios and spatial distributions of users, all helping to dimension the advanced cellular systems of today [38, 21]. As proximal communications is being steadily introduced to the contemporary cellular landscape, stochastic geometry is expected to play a pivotal role in its assessment, as it has the potential to efficiently characterize the uncertainty in locations of all the participating D2D users.

Therefore, a large number of studies addressing various D2D-centric scenarios by applying methods of stochastic geometry have already been published. The challenges of D2D link selection and base station assignment have been addressed by [39] utilizing a comprehensive modeling framework. The authors considered two different choices of frequencies for D2D communications – orthogonal and non-orthogonal. Using a Poisson Point Process (PPP) as the distribution of mobile devices, they developed an analytical methodology allowing to calculate user data rates in all of the considered cases. The paper in question demonstrated that for a high proportion of D2D-capable users the optimal division of spectrum in the overlay mode is invariant. Moreover, an important trade-off between the D2D selection threshold and the spectrum available for D2D communications has also been revealed, that is, the more D2D links are allowed to be established the less spectrum should be available for them to limit the resulting interference and vice versa. This useful framework has been extended subsequently in [40], where the authors applied stochastic geometry to develop centralized and distributed power control algorithms. The said work concluded that even though the centralized control outperforms the distributed alternative, the latter is also feasible.

Further, the authors in [41] addressed the D2D-aware power allocation problem. Here, the PPP has been used

to characterize the distribution of the transmit powers and the corresponding SINR for a D2D-enabled cellular network equipped with a power control capability. An important feature of this study is in that the omni-directional coverage areas of transmitters were allowed to intersect. Unfortunately, no optimization problem has been formulated to this end and thus no results on the optimal power allocation have been reported. Then, the comparison between the coordinated and the distributed scheduling of D2D transmissions has been considered by [42], where the SNR metric was employed to demonstrate the superiority of the former scheduling option. The underlying model was again based on a Poisson distribution of base stations with coverage areas induced by the respective Dirichlet tessellations resulting in formation of the Voronoi cells. The D2D transmitters have been assumed to all have omni-directional coverage areas and follow another PPP. The primary difference of this research compared to other studies is in that the associated receivers have been positioned at fixed worst-case distances from their transmitters. However, no particular mechanism for distributed coordination has been proposed.

A scenario of opportunistic D2D communications with orthogonal spectrum allocation and devices capable of energy harvesting has been studied in [43]. The authors modeled their base station positions by utilizing a PPP with the induced Voronoi cells characterizing the coverage of each base station. In this environment, the distribution of SIR has been obtained for both random and prioritized spectrum access. Another use case of opportunistic D2D communications has been investigated by [44]. The work in question employed the classical results from stochastic geometry to develop a simple control technique, where the D2D links are activated whenever the estimated target SIR on a link is above a certain preset threshold. Finally, the D2D coverage model that includes the power control capability can be found in [40, 45].

The above short summary of D2D-related work is by no means exhaustive. Still it confirms the applicability of stochastic geometry as a prominent tool for assessing the performance of network-assisted D2D systems. In contrast to all the discussed models, which for the most part focus on various open-space environments, *in this paper* we address an important practical scenario of D2D communications in adjacent rectangularly-shaped cells (e.g., rooms). This scenario is common for the urban areas with high user density, where D2D capabilities would be most needed, such as shopping malls, dormitories, offices, etc. In these environments, the presence of walls between the adjacent cells promises desirable conditions for communication between the D2D partners and may lead to simpler forms of assistance from the controlling base station, which may be limited solely to low-complexity classification of users across different areas of interest. In what follows, we characterize this novel type of D2D environment by employing both SIR and Shannon rate

metrics that reveal the effects of different wall materials on the resulting performance.

3. CONSIDERED SYSTEM MODEL

In this work, we focus on a high-density indoor metropolitan-type D2D deployment, where a floor of a building (e.g., a shopping mall or office) serves as the area of interest, see Fig. 2. This conventional shopping mall or office scenario naturally implies that the wireless cells all have rectangular shapes, and a single cell covers every room completely. In general, the potential D2D partners are assumed being distributed inside the cells randomly and uniformly. When communicating in the D2D mode, the transmitting devices take advantage of the omni-directional radiation pattern. In what follows, we do not focus on any specific D2D technology, as there may be several options for the latter (see above). Instead, all involved D2D users are assumed to share the same set of frequencies, that is, we consider the interference scenario where all the devices are assigned an identical set of communication channels or resource blocks across different cells to maximize the degrees of spatial reuse [46] and, thus, increase maximum upload speed [47].
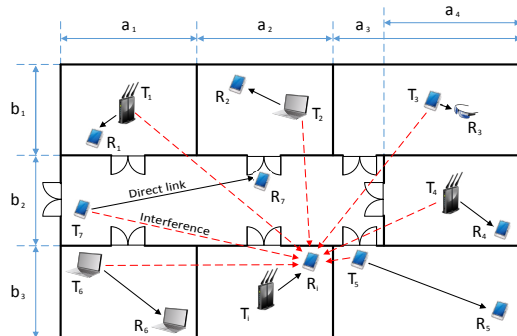

Figure 2. The considered D2D deployment in a city mall.

In what follows, we concentrate on two adjacent cells assuming that there is a single D2D pair operating in each of those at a time (as e.g., assigned by some network assistance function). For this scenario, we propose two performance approximation methods (see Fig. 3), where black solid lines indicate the data paths between the transmitters and their associated receivers, whereas red dashed lines correspond to the interfering signals from the neighboring transmitter. The reason behind offering two approximate models is in that the direct analysis of the target setup is extremely complex due to the uncertainty in locations of all the involved communicating entities.

In our first approximation, we assume that the receiving devices are positioned in the geometrical centers of their cells while the transmitting devices are allowed to be uniformly distributed within the respective cells. The second model is "mirrored", where the transmitting devices

are fixed at the cell centers and the receiving devices are distributed uniformly. For convenience, we refer to these approximations as to the "uplink" and "downlink" cases, respectively. As demonstrated in Fig. 3, both these models are expected to deliver a strict upper bound on the SIR performance, given that the fixed locations of either transmitters or receivers "protect" from extremely unfavorable user positions. For each of the two models, we further obtain the SIR distribution as a function of the important input parameters, including (i) the dimensions of cells a and b, and (ii) the propagation exponents on the direct and interference paths α_1 and α_2.

4. PROPOSED PERFORMANCE EVALUATION

4.1. SIR-centric considerations

To begin with, the SIR can be formally written as

$$S = \frac{P_{Rx}}{\sum_{i=1}^{N} I_i}, \qquad (1)$$

where the received signal power P_{Rx} is a function of the distance between the transmitter and the receiver, whereas the interference power I_i is a function of the distance and the signal between the receivers and the ith interfering user. In this paper, we consider SIR instead of the signal-to-interference-plus-noise ratio due to the fact that adding a constant factor to the denominator of the above function does not alter the underlying probabilistic behavior of the problem at hand, but the resulting expressions take a somewhat more complex form.

Further, the propagation model can be specified as

$$P = P(l_1) = g l_1^{-\alpha_1}, \ I_i = I_i(l_i) = g l_i^{-\alpha_i}, \qquad (2)$$

where g is the transmit power (assumed to be constant for all the transmitters), l_1 is the distance between the transmitter and the receiver, $l_i, \ i = 2, 3, \ldots, N$ are the distances between the interfering users and the receiver, and $\alpha_i, \ i = 1, 2, \ldots, N$ are the corresponding path loss exponents. For our scenario, the typical values of α_1 are around 2 corresponding to the line-of-sight transmission. Generally, the values of $\alpha_i, \ i = 2, 3, \ldots, N$ may vary from 2 to 6 depending on the material of walls between the cells as well as other details of propagation environment [48].

Both proposed models can in principle be treated similarly and we exemplify our approach by considering the "uplink" case shown in Fig. 3(a). To this end, we focus on a pair of users in the adjacent rectangular cells with the side lengths of (a_1, b_1) and (a_2, b_2), respectively. The receiver of interest (denoted as Rx_1) is equidistant from the edges of the tagged cell and the coordinates of the corresponding receiver are distributed uniformly over the area of this cell. The adjacent cell is associated with the transmitter Tx_1 and the receiver Rx_1 that use the same set of frequencies for their communication. Hence, we concentrate on the SIR at Rx_1. Let us then denote the
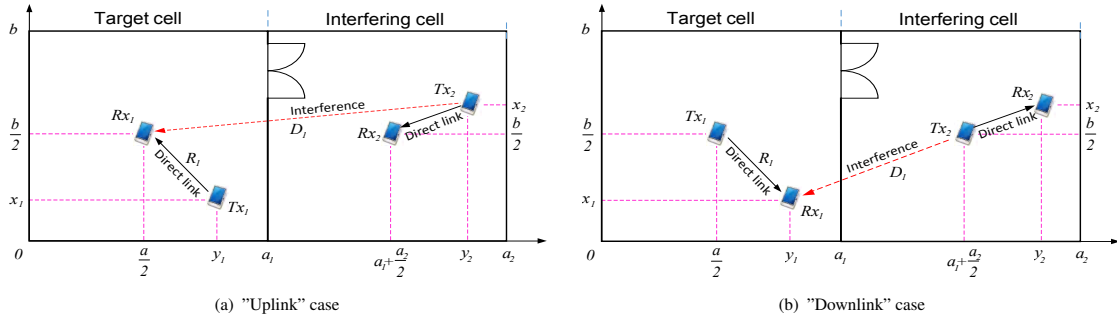
Figure 3. The proposed approximations for the target D2D scenario.

distance between the transmitter Tx_1 and the receiver Rx_1 as R_1, and the distance between Tx_2 and Rx_1 as D_1. Then, (1) can be written as

$$S = \frac{P_{Rx}(R_1)}{I(D_1)}, \qquad (3)$$

where $P_{Rx}(R_1) = gR_1^{-\alpha_1}$, $I(D_1) = gD_1^{-\alpha_2}$.

Assuming a constant transmit power, (3) reads as

$$S = \frac{R_1^{-\alpha_1}}{D_1^{-\alpha_2}} = R_1^{-\alpha_1} D_1^{\alpha_2}, \qquad (4)$$

thus producing the sought expression for the SIR analysis.

4.2. The overall procedure

The general methodology that we employ to establish the SIR distribution for the "downlink" and the "uplink" models is based on systematic application of the functional transformations of random variables, which are considered in detail in Appendix A. In both "downlink" and "uplink" cases the initial random variables are the coordinates of the interacting users. Successive application of the transformation technique allows to get distributions of functions of these coordinates including distance and SIR densities.

First, consider the "uplink" setup illustrated in Fig. 3(a), where the random user in the neighboring cell acts as interferer for the tagged central device. Due to the non-random receiver position, the interference path is independent from the useful signal path. In this case, we can readily estimate the distributions of the numerator and the denominator in the SIR expression (4), and then find the distribution of their ratio. The later step is feasible due to independence of propagation paths. Indeed, in order to obtain the distribution of the ratio between two random

variables we need to know their joint distribution, see Appendix A. In the "uplink" case (see Fig. 3(a)), due to the abovementioned independence property, the joint density is simply given by the product of the respective densities.

Interestingly, the "downlink" case leads to a more complicated analysis, as we cannot apply the "uplink" approach directly here – the two propagation paths are no longer independent from each other. While it is still feasible to determine the distributions of the numerator and the denominator separately, their joint density, which is required to then obtain the distribution of their ratio, is significantly harder to derive. **Nevertheless, the analysis is still feasible according to the generic procedure sketched in Appendix A and the summary of notation could be found in Table I.**

4.3. Detailed SIR analysis

The results summarized in this subsection have been obtained after applying our proposed approach introduced in the previous subsection. In addition, the transformation of random variables technique sketched in Appendix has been employed. Omitting the intermediate technical steps, for the "downlink" case we obtain the probability density function (pdf) of SIR in the form

$$S_D(x) = \int_0^\infty \mathbf{1}_{\mathbf{\Omega}_D}(x, y_2) W(x, y_2) dy_2, \qquad (5)$$

where

$$\mathbf{1}_{\mathbf{A}}(x, y) = \begin{cases} 1, (x, y) \in \mathbf{A} \\ 0, (x, y) \notin \mathbf{A} \end{cases} \qquad (6)$$

and the integrand is given by (7), which is is integrated over the domain $\mathbf{\Omega}_D = \Omega_{D,1} \cup \Omega_{D,2} \cup \Omega_{D,3} \cup \Omega_{D,4}$ presented in (8). Therefore, we have

$$W_D(y_1, y_2) = \frac{4}{c^2} \frac{y_1^{\frac{1}{\alpha_1}} y_2^{\frac{\alpha_2}{\alpha_1}+1}}{\sqrt{2c^2(y_1^{\frac{2}{\alpha_1}} y_2^{\frac{2\alpha_2}{\alpha_1}} + y_2^2) - (y_1^{\frac{2}{\alpha_1}} y_2^{\frac{2\alpha_2}{\alpha_1}} - y_2^2)^2 - c^4}} \qquad (7)$$

Table I. Simulation Parameters

Notation	Description
N	Number of interfering pairs
SIR, S	Signal-to-Interference ratio
R_1	Distance between target pair: receiver and transmitter
D_1	Distance between target receiver and interferer
Rx_1	Target receiver
Rx_2	Interfering cell receiver
Tx_1	Target transmitter
Tx_2	Interfering transmitter
$I_i, i=1,2,\ldots,N$	Interference power from the ith source
$l_i, i=1,2,\ldots,N$	Distance between the transmitter and the receiver
$\alpha_i, i=2,3\ldots,6$	Path loss exponent
g	Transmit power
$a_i = b_i = A, i=1,2,\ldots,N$	Cluster side length
P_{Rx}	Useful signal received power at the target receiver
S_D, S_U	Probability density function (pdf) of SIR
$S_{D,dB}, S_{U,dB}$	Logarithmic transformation of the value of SIR
$W_D, W_{U,i}, i=1,2,\ldots,6$	SIR probability density function (pdf)
Ω_D	Domain of integration
R	Achievable data rate in bits per second
C	Channel capacity in bits per second
w	Channel bandwidth

$$\Omega_{D,1} = \left\{ (y_1, y_2) : \frac{c}{2} \leq y_1^{\frac{1}{\alpha_1}} y_2^{\frac{\alpha_2}{\alpha_1}} \leq \frac{c}{\sqrt{2}}\ ,\ c - y_1^{\frac{1}{\alpha_1}} y_2^{\frac{\alpha_2}{\alpha_1}} \leq y_2 \leq y_1^{\frac{1}{\alpha_1}} y_2^{\frac{\alpha_2}{\alpha_1}} \right\}, \tag{8}$$

$$\Omega_{D,2} = \left\{ (y_1, y_2) : \frac{c}{\sqrt{2}} \leq y_1^{\frac{1}{\alpha_1}} y_2^{\frac{\alpha_2}{\alpha_1}} \leq c\ , c - y_1^{\frac{1}{\alpha_1}} y_2^{\frac{\alpha_2}{\alpha_1}} \leq y_2 \leq \sqrt{c^2 + y_1^{\frac{2}{\alpha_1}} y_2^{\frac{2\alpha_2}{\alpha_1}} - \sqrt{4c^2 y_1^{\frac{2}{\alpha_1}} y_2^{\frac{2\alpha_2}{\alpha_1}} - c^4}} \right\},$$

$$\Omega_{D,3} = \left\{ (y_1, y_2) : c \leq y_1^{\frac{1}{\alpha_1}} y_2^{\frac{\alpha_2}{\alpha_1}} \leq \frac{3c}{2}\ , y_1^{\frac{1}{\alpha_1}} y_2^{\frac{\alpha_2}{\alpha_1}} - c \leq y_2 \leq \sqrt{c^2 + y_1^{\frac{2}{\alpha_1}} y_2^{\frac{2\alpha_2}{\alpha_1}} - \sqrt{4c^2 y_1^{\frac{2}{\alpha_1}} y_2^{\frac{2\alpha_2}{\alpha_1}} - c^4}} \right\},$$

$$\Omega_{D,4} = \left\{ (y_1, y_2) : \frac{3c}{2} \leq y_1^{\frac{1}{\alpha_1}} y_2^{\frac{\alpha_2}{\alpha_1}} \leq \sqrt{\frac{5}{2}}c\ , \sqrt{y_1^{\frac{2}{\alpha_1}} y_2^{\frac{2\alpha_2}{\alpha_1}} - 2c^2} \leq y_2 \leq \sqrt{c^2 + y_1^{\frac{2}{\alpha_1}} y_2^{\frac{2\alpha_2}{\alpha_1}} - \sqrt{4c^2 y_1^{\frac{2}{\alpha_1}} y_2^{\frac{2\alpha_2}{\alpha_1}} - c^4}} \right\}.$$

Note that since we have to calculate the joint probability density function (jpdf) of the two propagation paths first, the domain of the integrand cannot be obtained in an explicit form. As a consequence, the integration limits for y_2 in (5) are defined by using the indicator function (6). Importantly, the result in (5) offers the pdf of the ratio between the received and the interfering power. To obtain a more typical logarithmically-scaled variable (expressed in dB), we have to apply another transform given by

$$S_{D,dB}(x) = S_D(10^{x/10})10^{x/10-1} \ln 10. \tag{9}$$

For the simpler "uplink" case, where the propagation paths are independent of each other, lets us obtain the integration limits in an explicit form. Nevertheless, to simplify the notation we still resort to using the indicator function. As a result, the SIR densities in the "uplink" setup are

$$S_U(x) = \int_0^\infty \sum_{i=1}^6 \mathbf{1}_{\Omega_{U,i}}(x, y_2)\, W_{U,i}(x, y_2) dy_2,$$

$$S_{U,dB}(x) = S_U(10^{x/10})10^{x/10-1} \ln 10, \tag{10}$$

where the components above are given by (11)–(12) below.

$$W_{U,1}(y_1, y_2) = A \arcsin \beta \left(\arcsin \gamma - \arcsin \delta \right), \ (y_1, y_2) \in \Omega_{U,1},$$

$$W_{U,2}(y_1, y_2) = \frac{\pi A}{2} \arcsin \beta, \ (y_1, y_2) \in \Omega_{U,2},$$

$$W_{U,3}(y_1, y_2) = A \arcsin \epsilon \left(\arcsin \gamma - \arcsin \delta \right), \ (y_1, y_2) \in \Omega_{U,3},$$

$$W_{U,4}(y_1, y_2) = \frac{\pi A}{2} \arcsin \epsilon, \ (y_1, y_2) \in \Omega_{U,4},$$

$$W_{U,5}(y_1, y_2) = A \left(\arcsin \epsilon - \arcsin \zeta \right) \left(\arcsin \gamma - \arcsin \delta \right), \ (y_1, y_2) \in \Omega_{U,5},$$

$$W_{U,6}(y_1, y_2) = \frac{\pi A}{2} \left(\arcsin \epsilon - \arcsin \zeta \right), \ (y_1, y_2) \in \Omega_{U,6} \tag{11}$$

and the coefficients in (11) are

$$A = \frac{8 y_2^{\frac{2}{\alpha_1}}}{\alpha_1 \alpha_2 c^4} (y_1 y_2)^{\frac{2}{\alpha_2} - 1},$$

$$\beta = \frac{\sqrt{-c^2 + 4(y_1 y_2)^{\frac{2}{\alpha_2}}}}{2(y_1 y_2)^{\frac{1}{\alpha_2}}},$$

$$\gamma = \frac{c}{2 y_2^{1/\alpha_1}},$$

$$\delta = \frac{\sqrt{-c^2 + 4 y_2^{2/\alpha_1}}}{2 y_2^{1/\alpha_1}},$$

$$\epsilon = \frac{c}{2(y_1 y_2)^{1/\alpha_2}},$$

$$\zeta = \frac{\sqrt{-9c^2 + 4(y_1 y_2)^{2/\alpha_2}}}{2(y_1 y_2)^{1/\alpha_2}}, \tag{12}$$

where the domains of integration are defined by (13) and (14).

We finally note that by setting $\alpha_1 = \alpha_2 = \alpha$, that is the provided expressions become significantly simpler considering D2D communications in an open-space environment. Similarly, when α_1 and α_2 are integers, the integrals in (5) and (10) can be expanded to obtain the sought solution in an explicit form

$$\Omega_{U,1} = \left\{ \Psi_7 \le y_1 \le \frac{\Psi_2}{\Psi_1}, \frac{\Psi_2}{y_1} \le y_2 \le \Psi_3 \right\} \cup \left\{ \frac{\Psi_2}{\Psi_1} < y_1 \le \frac{\Psi_3}{\Psi_4}, \Psi_1 \le y_2 \le \Psi_3 \right\} \cup \left\{ \frac{\Psi_3}{\Psi_4} < y_1 \le \frac{\Psi_4}{\Psi_1}, \Psi_1 \le y_2 \le \frac{\Psi_4}{y_1} \right\},$$

$$\Omega_{U,2} = \left\{ \frac{\Psi_2}{\Psi_1} \le y_1 \le \frac{\Psi_4}{\Psi_1}, \frac{\Psi_2}{y_1} \le y_2 \le \Psi_1 \right\} \cup \left\{ y_1 > \frac{\Psi_4}{\Psi_1} \cap \frac{\Psi_2}{y_1} \le y_2 \le \frac{\Psi_4}{y_1} \right\},$$

$$\Omega_{U,3} = \left\{ \frac{\Psi_3}{\Psi_4} \le y_1 \le \frac{\Psi_4}{\Psi_1}, \frac{\Psi_4}{y_1} \le y_2 \le \Psi_3 \right\} \cup \left\{ \frac{\Psi_4}{\Psi_1} < y_1 \le \frac{\Psi_7}{3^{-\alpha_2}}, \Psi_1 \le y_2 \le \Psi_3 \right\} \cup \left\{ \frac{\Psi_7}{3^{-\alpha_2}} < y_1 \le \frac{\Psi_5}{\Psi_1}, \Psi_1 \le y_2 \le \frac{\Psi_5}{y_1} \right\},$$

$$\Omega_{U,4} = \left\{ \frac{\Psi_4}{\Psi_1} \le y_1 \le \frac{\Psi_5}{\Psi_1}, \frac{\Psi_4}{y_1} \le y_2 \le \Psi_1 \right\} \cup \left\{ \frac{\Psi_5}{\Psi_1} < y_1, \frac{\Psi_4}{y_1} \le y_2 \le \frac{\Psi_5}{y_1} \right\},$$

$$\Omega_{U,5} = \left\{ \frac{\Psi_5}{\Psi_3} \le y_1 \le \Psi_8, \frac{\Psi_5}{y_1} \le y_2 \le \Psi_3 \right\} \cup \left\{ \Psi_8 < y_1 \le \frac{\Psi_5}{\Psi_1}, \frac{\Psi_5}{y_1} \le y_2 \le \frac{\Psi_6}{y_1} \right\} \cup \left\{ \frac{\Psi_5}{\Psi_1} < y_1 \le \frac{\Psi_6}{\Psi_1}, \Psi_1 \le y_2 \le \frac{\Psi_6}{y_1} \right\},$$

$$\Omega_{U,6} = \left\{ \frac{\Psi_5}{\Psi_1} \le y_1 \le \frac{\Psi_6}{\Psi_1}, \frac{\Psi_5}{y_1} \le y_2 \le \Psi_1 \right\} \cup \left\{ \frac{\Psi_6}{\Psi_1} < y_1, \frac{\Psi_5}{y_1} \le y_2 \le \frac{\Psi_6}{y_1} \right\}. \tag{13}$$

$$\Psi_1 = \left(\frac{c}{2} \right)^{\alpha_1}, \qquad \Psi_5 = \left(\frac{3c}{2} \right)^{\alpha_2},$$

$$\Psi_2 = \left(\frac{c}{2} \right)^{\alpha_2}, \qquad \Psi_6 = c^{\alpha_2} \left(\sqrt{\frac{5}{2}} \right)^{\alpha_2},$$

$$\Psi_3 = \left(\frac{c}{\sqrt{2}} \right)^{\alpha_1}, \qquad \Psi_7 = \frac{c^{\alpha_2 - \alpha_1}}{\left(\sqrt{2} \right)^{2\alpha_2 - \alpha_1}},$$

$$\Psi_4 = \left(\frac{c}{\sqrt{2}} \right)^{\alpha_2}, \qquad \Psi_8 = c^{\alpha_2 - \alpha_1} \sqrt{\frac{5^{\alpha_2}}{2^{\alpha_2 - \alpha_1}}}. \tag{14}$$

5. MAIN NUMERICAL RESULTS

In this section, we first validate the obtained quantitative data with our developed simulation environment. In connection to this, we thoroughly assess the accuracy of our proposed approximations by comparing the respective results with those produced by simulations. Further, we investigate numerically the response of both the "uplink" and the "downlink" models with respect to the key input parameters. Finally, we demonstrate how these proposed models could be used for the actual D2D data rate analysis.

Table II. Simulation Setup

Parameter	Description
$a = b = c \in [5; 25]$	Cluster side length
$\alpha_1 = 2$	Target cluster path loss exponent
$\alpha_2 \in [2; 6]$	Interfering clusters path loss exponent
$w = 180$ kHz	Channel bandwidth
$\bar{a} = 1.2456, \bar{b} = 1.3463$	Fitting parameters of the modified Shannon's expression
10^6	Number of samples
200	Sampling frequency
Log-distance path loss model	Propagation model

System parameters and their values used in this section are shown in Table II.

5.1. Validation and accuracy of our approximation

To carefully validate our proposed approximations as well as to assess their accuracy in the target D2D communications scenario, where all the considered transmitters and receivers are distributed randomly and uniformly in their respective cells, we develop a simple yet powerful simulator based on direct modeling of the involved random variables and the subsequent estimation of the associated performance metrics. Our developed simulator allows varying all of the input parameters of interest accounted for by the studied system model, including the dimensions of the cells a and b, the path loss exponents α_1 and α_2, the number of experiments, and the sampling frequency. As an output, our tool provides the empirical density functions, the sample means and standard deviations, as well as the estimates of the quantiles of the main random variables, such as SIR and Shannon rate.

Along these lines, Fig. 4 compares the analytical results against those obtained with simulations for the "uplink" and the "downlink" scenarios. In both cases, the dimensions of the cells are set as $a = b = c = 10$, whereas various path loss exponents are used on different paths. The number of samples used to construct the empirical densities has been taken as $10e6$. As a result, the simulation data indicates the excellent match with the respective analytical results. For both models, the Kolmogorov-Smirnov goodness-of-fit statistical test [49] has been performed with the level of significance set to 0.05. This confirms the hypothesis on that the simulation samples belong to our considered analytical distribution.

Analyzing the results shown in Fig. 4 further, we notice that both proposed models provide a somewhat loose estimation of the empirical SIR density in our characteristic D2D scenario. The underlying reason is that for both approximations we restrict the locations of either transmitter or receiver to the geometrical center of a cell and thus "disable" any potential worst-case positioning options of transmitters/receivers with respect to each other. Therefore, whereas our models could be insufficiently accurate to characterize the quantiles of SIR, they might be very useful to capture the moments of the target metrics of interest. In this regard, we particularly highlight the behavior of our "uplink" model that essentially mimics the performance of the D2D system, while at the same time maintains the much needed operational simplicity and low computational complexity.

To conclusively assess whether our proposed approximate models could reflect the D2D scenario under investigation, Fig. 5 provides the mean and the standard deviation of SIR over a broad range of path loss exponents α_2 between the interferer and the receiver. As we observe, both the "uplink" and the "downlink" models yield an upper bound of SIR, implying that any of those may be used as a first-order optimistic estimate on the achievable SIR. Importantly, the absolute approximation error for the mean value decreases with the growth of α_2 from around 2.2 dB for $\alpha_2 \in (2, 3)$ to as low as 1.4 dB for $\alpha_2 > 4$. In our calculations, we assume that the highest effective SIR value is 30 dB and increasing it further would not bring any substantial D2D performance benefits. This is due to the fact that the values of SIR over 20 dB lead to the use of the best possible modulation and coding schemes; hence any further data rate improvement is not possible for higher SIR [50]. In practice, unnecessarily large SIR values can be controlled by employing various techniques similar to reduction in the device transmit power.

5.2. Properties of the proposed models

Our proposed approximate models have a number of curious properties that may simplify the D2D performance analysis for different configurations of cells. In particular, the SIR density function and, therefore, all the associated moments are insensitive to the choice of the cell dimensions a and b, when $a = b$ and $\alpha_1 = \alpha_2$. This conclusion follows directly from the utilized methodology and is particularly important for the open-space environments. Another interesting feature is the *scaling* of the studied density functions, when the same path loss exponents are assumed on both the signal and the interference paths. This useful finding is illustrated in Fig. 6, which shows the "uplink" and the "downlink" densities for $a = b = c = 5, 15, 25$ with $\alpha_1 = 2$ and $\alpha_2 = 3$.
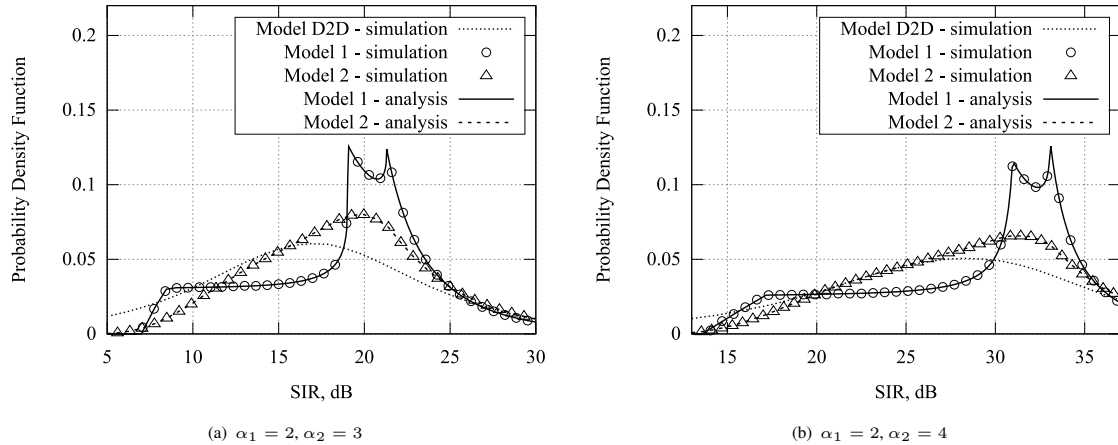
Figure 4. Analytical and simulated SIR densities for the proposed models, $a = b = c = 10$.
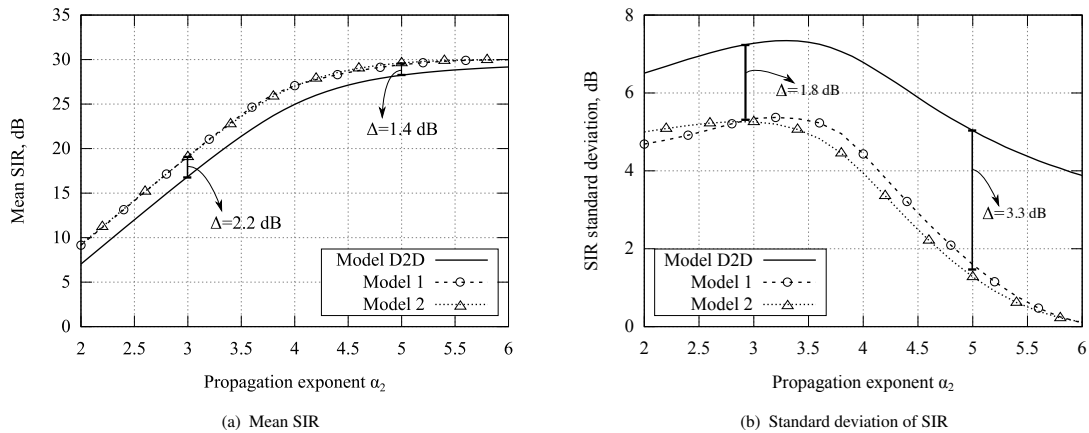

Figure 5. Analytical and simulated SIR moments for the proposed models, $a = b = c = 10$, $\alpha_1 = 2$.

Furthermore, Fig. 7 demonstrates the impact of different values of α_2 for the identical cell dimensions $a = b = c = 10$. As we learn from the figure, this effect is fairly straightforward and self-explanatory: the larger the α_2 is, the better the interference picture at the receiver side becomes. Recalling that the value of α_2 is primarily determined by the material of walls, our proposed models allow for capturing the SIR properties for different construction materials.

5.3. D2D performance analysis

Let us finally offer a simple numerical example characterizing the performance of D2D communications within the licensed LTE band. We remind that a single LTE resource block of bandwidth is 180 kHz which is assumed to be reused across the neighboring cells. To estimate the achievable data rate, we employ the modified Shannon's

formula in the form

$$R = \frac{w}{\bar{b}} \log_2 \left(1 + \frac{SIR}{\bar{a}} \right), \quad (15)$$

where $w = 180$ kHz is the channel bandwidth, while $\bar{a} = 1.2456$ and $\bar{b} = 1.3463$ are the fitting parameters of the modified Shannon's expression for 3GPP LTE systems borrowed from [51].

Given that our obtained SIR is a random variable, and in accordance with (15), we apply the following transformation utilizing it to produce the mean and the standard deviation of the channel capacity estimate C

$$C = S_i \left[\bar{a}(2^{\bar{b}x/w} - 1) \right] 2^{\bar{b}x/w} \frac{\bar{a}\bar{b} \ln 2}{w}, i \in D, U. \quad (16)$$

In light of the above, Fig. 8 demonstrates the mean D2D data rate achieved over a single resource block in adjacent cells, as well as the corresponding standard deviation of
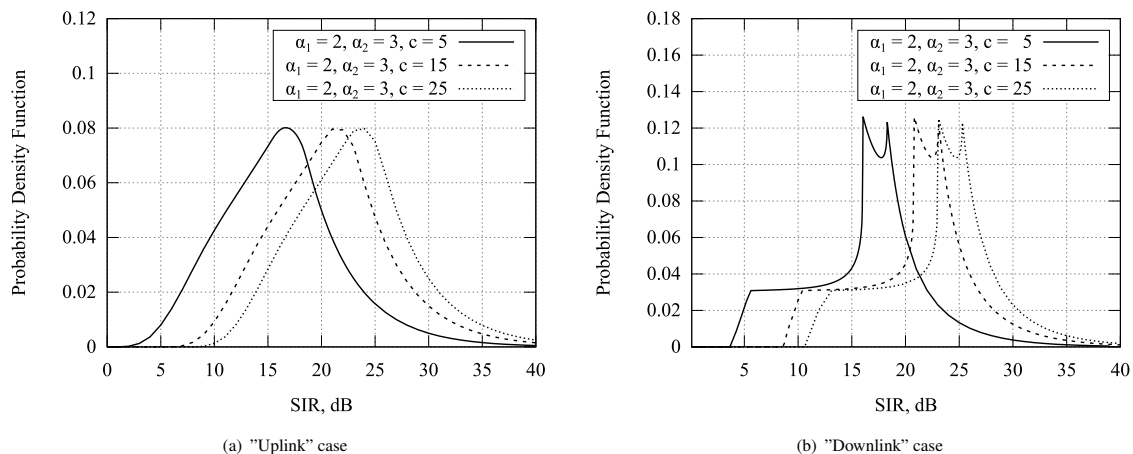
(a) "Uplink" case

(b) "Downlink" case

Figure 6. The scaling effects of cell dimensions.
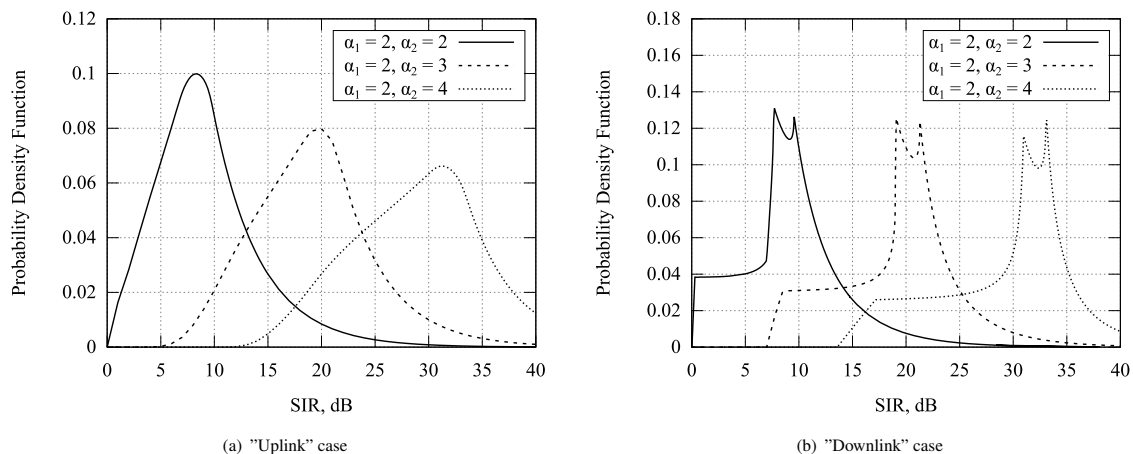

(a) "Uplink" case

(b) "Downlink" case

Figure 7. The effects of different α_2 for $a = b = c = 10$.

this rate. We note that the difference between our simulated D2D scenario and the considered approximate models is typically around 10% and decreases further with the growth of the path loss exponent α_2. Therefore, the upper bound delivered by the proposed D2D performance estimations is acceptable for the overall data rate assessment.

6. SUMMARY AND CONCLUSIONS

In this work, we analyzed the emerging concept of D2D communications in a characteristic urban scenario with rectangular cells. Our proposed modeling framework is a powerful tool to estimate the SIR and the data rate distributions analytically without the need for time-consuming and often prohibitive system-level simulations. Both considered mathematical models, named "uplink" and "downlink", provide reasonable upper bounds on the respective

system performance showing the accuracy of about 10% according to the respective simulation data. Comparing the results produced by these two models, we conclude that even though they lead to different distributions, the output mean SIR values are nearly identical. Hence, for most practical purposes, we recommend the application of the simpler "uplink" method resulting in lower complexity. Further, as the gap between the reported analytical and simulation data is near-constant, one may properly adjust the model in question to deliver even tighter SIR and data rate estimates. Interestingly, the dependence of our results on the propagation exponent is linear for both SIR and data rate.

Extending the proposed simple approximations for the real-world D2D scenario, where both communicating devices of interest assume arbitrary locations, another pair of random coordinates has to be introduced. This, in turn, will invoke all the underlying mathematical manipulations,
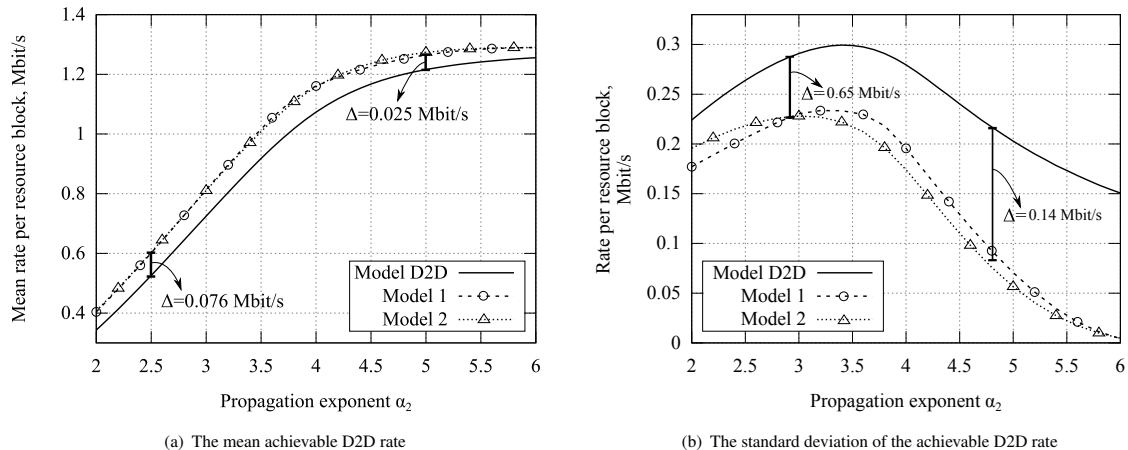
(a) The mean achievable D2D rate

(b) The standard deviation of the achievable D2D rate

Figure 8. The mean and the standard deviation of the achievable D2D rate.

beginning with the jpdf calculation for the two corresponding propagation paths, which would yield significantly more involved derivations. To this end, one of the possible solutions is to assume these paths to be independent from each other, which might lead to adequate approximations, but would still suffer from the associated analytical complexity. Therefore, our proposed modeling approach maintains attractive balance between the incurred mathematical complexity and the resulting performance. Finally, we believe that the methodology presented in this paper may also be useful in a more general context of heterogeneous networks – both "uplink" and "downlink" cases can thus be reused subject to the necessary modifications.

We plan to continue our efforts by characterizing D2D scenarios where more than one cell affects the transmission. As for our preliminary investigations, we demonstrate that while those models presented in the paper are accurate for two adjacent cells they are more biased for multi-cell scenarios featuring 8 cells at one floor or 26 cells in 3D-space at the floor of interest (9 and 9 at floors above and below and 8 at the floor having the tagged cell). However, we observed that the effect of dependence between propagation paths we highlighted in the paper vanishes when more interfering cells are taken into account. This is of special interest as it allows for simple analysis of more complex system configurations.

A. DISTRIBUTIONS OF FUNCTIONS OF RANDOM VARIABLES

According to [52, 53], we review below a solution to the generic problem of obtaining the joint distribution of a number of random variables (RVs) specified as functions of a certain number of other RVs. These important results are employed in subsection 4.3 above to produce the

SIR distributions in both the "uplink" and the "downlink" cases.

First, consider the general case and let $\boldsymbol{\xi} = (\xi_1, \xi_2, \ldots, \xi_n)$ be the set of RVs with the jpdf $w_{\boldsymbol{\xi}}(\boldsymbol{x})$. Then, suppose that the transformation for this set is given as

$$y_k = f_k(\boldsymbol{x}), \ k = \overline{1, n}. \tag{17}$$

Hence, we target to characterize the jpdf of n transformed RVs as a function of n initial RVs. When the resulting set of random variables has fewer elements than the initial set, we first need to introduce some auxiliary variables, such that both sets would have exactly the same number of RVs. The solution is then similar to what we outline below, except for the last step where we need to integrate over all the auxiliary RVs.

Further, using (17) we can obtain the jpdf $W_{\boldsymbol{\eta}}(\boldsymbol{y})$ of the new RVs $\boldsymbol{\eta} = (\eta_1, \eta_2, \ldots, \eta_n)$, where

$$\eta_k = f_k(\boldsymbol{\xi}), \ k = \overline{1, n}. \tag{18}$$

Let now

$$x_k = \phi_k(\boldsymbol{y}), \ k = \overline{1, n}, \tag{19}$$

be the inverse of (17). In general, ϕ_k is a multivalued function having a number of branches. Therefore, denote the i-th branch by

$$x_{k,i} = \phi_{k,i}(\boldsymbol{y}), \ k = \overline{1, n}, \ i \geq 1. \tag{20}$$

Observe that $\boldsymbol{\eta}$ can be considered as a point in the n-dimensional Euclidean space. To this end, define B as an event corresponding to when the point $\boldsymbol{\eta}$ falls into a certain n-dimensional subspace S_y. The probability of such an event comprises the contributions by all the branches of ϕ_k. Then, defining A_i as $\boldsymbol{\xi} \in S_{x_i}$, $i = 1, 2, \ldots$, we observe that $B = \cup_i A_i$ and $A_i \cap A_j = \emptyset$, $i \neq j$, which implies that the probability of the event B may be

A. Samuylov et al.

expressed as

$$P\{B\} = V_y = \sum_i V_{x_i} = \sum_i P\{A_i\}, \qquad (21)$$

where V_y is the n-dimensional volume. Assuming sufficiently small volumes of S_{x_i} and S_y, the expression for V_i can be approximated as follows

$$V_y \approx W_{\boldsymbol{\eta}}(\boldsymbol{y})S_y, \ V_{x_i} \approx w_{\boldsymbol{\eta}}(\boldsymbol{x}_i)S_{x_i}. \qquad (22)$$

The limit of the ratio S_{x_i}/S_y can then be expressed through a Jacobian as

$$J_i = \lim_{\substack{S_{x_i} \to 0 \\ S_y \to 0}} \frac{S_{x_i}}{S_y} = \frac{\partial(x_{1,i}, \dots, x_{n,i})}{\partial(y_1, \dots, y_n)} =$$

$$= \begin{vmatrix} \frac{\partial x_{1,i}}{\partial y_1} & \cdots & \frac{\partial x_{1,i}}{\partial y_n} \\ \vdots & & \vdots \\ \frac{\partial x_{n,i}}{\partial y_1} & \cdots & \frac{\partial x_{n,i}}{\partial y_n} \end{vmatrix}, \ i \geq 1. \qquad (23)$$

From (21)-(23), we express the sought jpdf as

$$W_{\boldsymbol{\eta}}(\boldsymbol{y}) = \sum_i w_{\boldsymbol{\xi}}(\phi_{1,i}(\boldsymbol{y}), \dots, \phi_{n,i}(\boldsymbol{y})) \, |J_i| \,. \qquad (24)$$

Consider now the scalar transformation function in the form

$$\boldsymbol{y} = (y_1), \ y_1 = f(x_1, \dots, x_n). \qquad (25)$$

By introducing the auxiliary variables as

$$y_k = x_k, \ k = \overline{2, n}, \qquad (26)$$

we first need to determine the jpdf of the following set of RVs

$$\eta_1 = f(\boldsymbol{\xi}), \ \eta_k = \xi_k, \ k = \overline{2, n}, \qquad (27)$$

with the known jpdf $w_{\boldsymbol{\xi}}(\boldsymbol{x})$.

In this case, it is easy to show that

$$x_1 = \phi(\boldsymbol{y}), \ x_k = y_k, \ k = \overline{2, n}, \ J_i = \frac{\partial \phi_i(\boldsymbol{y})}{\partial y_1}. \qquad (28)$$

According to (24), the required jpdf is readily given by

$$W_{\boldsymbol{\eta}}(\boldsymbol{y}) = \sum_i w_{\boldsymbol{\xi}}(\phi(\boldsymbol{y}), y_2, \dots, y_n) \left| \frac{\partial \phi_i(\boldsymbol{y})}{\partial y_1} \right|. \qquad (29)$$

Integrating over the auxiliary RVs, we receive the final form of the pdf $W_{\eta_1}(y_1)$ as

$$\sum_i \int_{\mathbf{Y}_i} w_{\boldsymbol{\xi}}(\phi(\boldsymbol{y}), y_2, \dots, y_n) \left| \frac{\partial \phi_i(\boldsymbol{y})}{\partial y_1} \right| \mathrm{d}y_n \dots \mathrm{d}y_2, \tag{30}$$

where $\mathbf{Y}_i$ is the domain of variables $y_2, \dots, y_n$ for the i-th branch.

REFERENCES

1. Cisco Visual Networking Index, "Global mobile data traffic forecast update, 2014-2019," *White Paper*, February 2015.
2. I. F. Akyildiz, D. M. Gutierrez-Estevez, and E. C. Reyes, "The evolution to 4G cellular systems: LTE-Advanced," *Physical Communication*, vol. 3, no. 4, pp. 217–244, 2010.
3. F. Boccardi, R. W. Heath Jr, A. Lozano, T. L. Marzetta, and P. Popovski, "Five Disruptive Technology Directions for 5G," *IEEE Communications Magazine*, vol. 52, no. 2, pp. 74–80, 2014.
4. L. Ericsson, "More than 50 billion connected devices," *White Paper*, 2011.
5. The 5G Infrastructure Public Private Partnership, "5G Vision: The next generation of communication networks and services," February 2015.
6. D. Raychaudhuri and N. B. Mandayam, "Frontiers of wireless and mobile communications," *Proceedings of the IEEE*, vol. 100, no. 4, pp. 824–840, 2012.
7. M. Condoluci, M. Dohler, G. Araniti, A. Molinaro, and K. Zheng, "Toward 5G densenets: architectural advances for effective machine-type communications over femtocells," *IEEE Communications Magazine*, vol. 53, no. 1, pp. 134–141, 2015.
8. Z. Zhou, M. Dong, K. Ota, J. Wu, and T. Sato, "Energy Efficiency and Spectral Efficiency Tradeoff in Device-to-Device (D2D) Communications," *arXiv preprint arXiv:1407.1556*, 2014.
9. S.-P. Yeh, S. Talwar, G. Wu, N. Himayat, and K. Johnsson, "Capacity and coverage enhancement in heterogeneous networks," *IEEE Wireless Communications*, vol. 18, no. 3, pp. 32–38, 2011.
10. P. Marsch, B. Raaf, A. Szufarska, P. Mogensen, H. Guan, M. Farber, S. Redana, K. Pedersen, and T. Kolding, "Future mobile communication networks: challenges in the design and operation," *IEEE Vehicular Technology Magazine*, vol. 7, no. 1, pp. 16–23, 2012.
11. F. H. Fitzek, M. Katz, and Q. Zhang, "Cellular controlled short-range communication for cooperative P2P networking," *Wireless Personal Communications*, vol. 48, no. 1, pp. 141–155, 2009.
12. K. Zheng, F. Hu, W. Wang, W. Xiang, and M. Dohler, "Radio resource allocation in LTE-advanced cellular networks with M2M communications," *IEEE Communications Magazine*, vol. 50, no. 7, pp. 184–192, 2012.
13. L. Militano, M. Condoluci, G. Araniti, A. Molinaro, and A. Iera, "When D2D communication improves group oriented services in beyond 4G networks," *Wireless Networks*, vol. 21, no. 4, pp. 1363–1377, 2014.

14. C.-H. Yu, K. Doppler, C. B. Ribeiro, and O. Tirkkonen, "Resource sharing optimization for device-to-device communication underlaying cellular networks," *IEEE Transactions on Wireless Communications*, vol. 10, no. 8, pp. 2752–2763, 2011.

15. G. Fodor, E. Dahlman, G. Mildh, S. Parkvall, N. Reider, G. Miklós, and Z. Turányi, "Design aspects of network assisted device-to-device communications," *IEEE Communications Magazine*, vol. 50, no. 3, pp. 170–177, 2012.

16. G. Fodor, S. Sorrentino, and S. Sultana, "Network Assisted Device-to-Device Communications: Use Cases, Design Approaches, and Performance Aspects," in *Smart Device to Smart Device Communication*. Springer, 2014, pp. 135–163.

17. A. Pyattaev, K. Johnsson, S. Andreev, and Y. Koucheryavy, "Communication Challenges in High-Density Deployments of Wearable Wireless Devices," *IEEE Wireless Communications Magazine*, vol. 22, no. 1, pp. 12–18, 2015.

18. S. Andreev, A. Pyattaev, K. Johnsson, O. Galina, and Y. Koucheryavy, "Cellular traffic offloading onto network-assisted device-to-device connections," *IEEE Communications Magazine*, vol. 52, no. 4, pp. 20–31, 2014.

19. G. R. Hendrey, H. A. Tanaka, and P. J. Koopman Jr, "Method and system for selectively connecting mobile users based on physical proximity," 2003, US Patent 6,542,750.

20. S. Weber, J. G. Andrews, and N. Jindal, "An overview of the transmission capacity of wireless networks," *IEEE Transactions on Communications*, vol. 58, no. 12, pp. 3593–3604, 2010.

21. J. G. Andrews, R. K. Ganti, M. Haenggi, N. Jindal, and S. Weber, "A primer on spatial modeling and analysis in wireless networks," *IEEE Communications Magazine*, vol. 48, no. 11, pp. 156–163, 2010.

22. D. Levine, I. F. Akyildiz, M. Naghshineh *et al.*, "A resource estimation and call admission algorithm for wireless multimedia networks using the shadow cluster concept," *IEEE/ACM Transactions on Networking*, vol. 5, no. 1, pp. 1–12, 1997.

23. D. Astely, E. Dahlman, G. Fodor, S. Parkvall, and J. Sachs, "LTE release 12 and beyond," *IEEE Communications Magazine*, vol. 51, no. 7, pp. 154–160, 2013.

24. K. Doppler, M. Rinne, C. Wijting, C. B. Ribeiro, and K. Hugl, "Device-to-device communication as an underlay to LTE-advanced networks," *IEEE Communications Magazine*, vol. 47, no. 12, pp. 42–49, 2009.

25. K. Doppler, J. Manssour, A. Osseiran, and M. Xiao, "Innovative concepts in peer-to-peer and network coding," *Celtic Telecommunication Solutions*, vol. 16, p. 09, 2008.

26. P. Stavroulakis, *Terrestrial trunked radio-TETRA: a global security tool*. Springer Science & Business Media, 2007.

27. T. Doumi, M. F. Dolan, S. Tatesh, A. Casati, G. Tsirtsis, K. Anchan, and D. Flore, "LTE for public safety networks," *IEEE Communications Magazine*, vol. 51, no. 2, pp. 106–112, 2013.

28. C.-H. Yu, O. Tirkkonen, K. Doppler, and C. Ribeiro, "Power optimization of device-to-device communication underlaying cellular communication," in *Proc. of IEEE International Conference on Communications (ICC)*, 2009, pp. 1–5.

29. Y. Li, K. K. Chai, Y. Chen, and J. Loo, "Duty cycle control with joint optimisation of delay and energy efficiency for capillary machine-to-machine networks in 5G communication system," *Transactions on Emerging Telecommunications Technologies*, vol. 26, no. 1, pp. 56–69, 2015.

30. X. Xu, H. Wang, H. Feng, and C. Xing, "Analysis of device-to-device communications with exclusion regions underlaying 5G networks," *Transactions on Emerging Telecommunications Technologies*, vol. 26, no. 1, pp. 93–101, 2015.

31. J.-B. Dore, V. Berg, and D. Ktenas, "Channel estimation techniques for 5G cellular networks: FBMC and multiuser asynchronous fragmented spectrum scenario," *Transactions on Emerging Telecommunications Technologies*, vol. 26, no. 1, pp. 15–30, 2015.

32. J. Perez-Romero, O. Sallent, R. Agusti, and L. Giupponi, "A novel on-demand cognitive pilot channel enabling dynamic spectrum allocation," in *2nd IEEE International Symposium on New Frontiers in Dynamic Spectrum Access Networks*. IEEE, 2007, pp. 46–54.

33. A. Pyattaev, K. Johnsson, A. Surak, R. Florea, S. Andreev, and Y. Koucheryavy, "Network-assisted D2D communications: Implementing a technology prototype for cellular traffic offloading," in *IEEE Wireless Communications and Networking Conference (WCNC)*. IEEE, 2014, pp. 3266–3271.

34. S. Andreev, D. Moltchanov, O. Galinina, A. Pyattaev, A. Ometov, and Y. Koucheryavy, "Network-Assisted Device-to-Device Connectivity: Contemporary Vision and Open Challenges," in *Proc. of 21th European Wireless Conference*. VDE, 2015, pp. 1–8.

35. L. Al-Kanj, Z. Dawy, W. Saad, and E. Kutanoglu, "Energy-aware cooperative content distribution over wireless networks: Optimized and distributed approaches," *IEEE Transactions on Vehicular Technology*, vol. 62, no. 8, pp. 3828–3847, 2013.

36. A. Ometov, K. Zhidanov, S. Bezzateev, R. Florea, S. Andreev, and Y. Koucheryavy, "Securing Network-Assisted Direct Communication: The Case of Unreliable Cellular Connectivity," in *Proc. of IEEE 14th International Conference on Trust, Security and Privacy in Computing and Communications (TrustCom)*. IEEE, 2015.

37. E. Yaacoub and Z. Dawy, "A survey on uplink resource allocation in OFDMA wireless networks,"

Communications Surveys & Tutorials, IEEE, vol. 14, no. 2, pp. 322–337, 2012.

38. M. Haenggi, J. G. Andrews, F. Baccelli, O. Dousse, and M. Franceschetti, "Stochastic geometry and random graphs for the analysis and design of wireless networks," *IEEE Journal on Selected Areas in Communications*, vol. 27, no. 7, pp. 1029–1046, 2009.

39. X. Lin, J. G. Andrews, and A. Ghosh, "Spectrum sharing for device-to-device communication in cellular networks," *IEEE Transactions on Wireless Communications*, vol. 13, no. 12, pp. 6727–6740, 2014.

40. N. Lee, X. Lin, J. G. Andrews, and R. Heath, "Power Control for D2D Underlaid Cellular Networks: Modeling, Algorithms, and Analysis," *IEEE Journal on Selected Areas in Communications*, vol. 33, no. 1, pp. 1–13, 2015.

41. M. C. Erturk, S. Mukherjee, H. Ishii, and H. Arslan, "Distributions of transmit power and SINR in device-to-device networks," *IEEE Communications Letters*, vol. 17, no. 2, pp. 273–276, 2013.

42. S. Stefanatos, A. G. Gotsis, and A. Alexiou, "Analytical Assessment of Coordinated Overlay D2D Communications," in *Proc. of 20th European Wireless*. VDE, 2014, pp. 1–6.

43. A. H. Sakr and E. Hossain, "Cognitive and energy harvesting-based D2D communication in cellular networks: Stochastic geometry modeling and analysis," *IEEE Transactions on Communications*, vol. 63, no. 5, pp. 1867–1880, 2015.

44. Z. Chen and M. Kountouris, "Distributed SIR-aware opportunistic access control for D2D underlaid cellular networks," in *Proc. of IEEE Global Communications Conference (GLOBECOM)*. IEEE, 2014, pp. 1540–1545.

45. Z. Liu, T. Peng, Q. Lu, and W. Wang, "Transmission capacity of D2D communication under heterogeneous networks with dual bands," in *Proc. of 7th International ICST Conference on Cognitive Radio Oriented Wireless Networks and Communications (CROWNCOM)*. IEEE, 2012, pp. 169–174.

46. L. Militano, A. Orsino, G. Araniti, A. Molinaro, A. Iera, and L. Wang, "Efficient Spectrum Management Exploiting D2D Communication in 5G Systems," *Proc. of IEEE International Symposium on Broadband Multimedia Systems and Broadcasting (BMSB)*, pp. 1–5, 17-19 June 2015.

47. *Efficient Data Uploading Supported by D2D Communications in LTE-A Systems*, 20-22 May 2015.

48. 3GPP, "3rd Generation Partnership Project; Technical Specification Group Radio Access Networks; Radio Frequency (RF) system scenarios (Release 9)," *Technical Report 25.942 v9.0.0*, 12-2009.

49. F. J. Massey Jr, "The Kolmogorov-Smirnov test for goodness of fit," *Journal of the American statistical Association*, vol. 46, no. 253, pp. 68–78, 1951.

50. Motorola, Inc., "TBS and MCS Signaling and Tables," *3GPP R1-081638*, April 2008.

51. O. Galinina, A. Trushanin, V. Shumilov, R. Maslennikov, Z. Saffer, S. Andreev, and Y. Koucheryavy, "Energy-efficient operation of a mobile user in a multi-tier cellular network," in *Analytical and Stochastic Modeling Techniques and Applications*. Springer, 2013, pp. 198–213.

52. B. Levin, *Theoretical Foundations of Statistical Radio Engineering*, 3rd ed. M.: Radio i Svyaz, 1989.

53. A. Mood, F. Graybill, and D. Boes, *Introduction to the theory of statistics*, 1st ed. McGraw-Hill, 1974.